Magnetic and hyperfine properties of fcc Fe

Diana Guenzburger
Centro Brasileiro de Pesquisas Físicas (CBPF), rua Dr. Xavier Sigaud, 150, 22290-180 Rio de Janeiro, RJ, Brazil

D. E. Ellis
Department of Physics and Astronomy and Materials Research Center, Northwestern University, Evanston, Illinois 60208
(Received 12 October 1994; revised manuscript received 7 February 1995)

First-principles electronic-structure calculations based on density-functional theory were performed for 62-atom embedded clusters representing fcc iron with antiferromagnetic and ferromagnetic spin structures. The results obtained indicate that the large difference observed experimentally in the magnitude of the hyperfine fields of antiferromagnetic and ferromagnetic γ-Fe originates mainly from different signs of the conduction electrons' contribution, and not from large differences in the Fe magnetic moment.

I. INTRODUCTION

Pure bulk fcc (γ) iron only exists at very high temperatures (between 1183 and 1667 K); however, fcc Fe may be stabilized down to very low temperatures either as small γ-Fe coherent precipitates in a Cu (Refs. 1–5) or Cu alloy (Refs. 6 and 7) matrix or as thin epitaxial films on a Cu substrate.[8,9] Recently, there has been great interest in investigating the properties of γ-Fe thus obtained, driven also by a number of band-structure calculations that showed, among other features, the existence of several magnetic states.[10–15] The relative stability of the different magnetic states depends critically on the lattice constant, as does the value of the Fe magnetic moment.[13] The existence of multiple magnetic states may be related to the properties of γ-Fe-based INVAR alloys.

Experimentally, variations in the lattice constant of fcc Fe may be obtained by substituting Cu by Cu alloys with components of larger atomic volume. Such a procedure was adopted for coherent γ-Fe precipitates and films in Cu-Au and Cu-Al alloys.[9] Pressure may be also used for further lattice constant variation.[9] By use of ^{57}Fe Mössbauer spectroscopy, the hyperfine field at the Fe nucleus has been measured for γ-iron precipitates in $Cu_{100-x}Al_x$ and thin films on Cu and Cu_3Au.[7–9] The results, summarized in Fig. 6 of Ref. 9, show that for small Wigner-Seitz radii small values of the hyperfine fields H_F are obtained (below 5 T); above approximately $r_s = 6.68$ a.u., the magnitude of H_F rises abruptly to values around 35 T. According to band-structure calculations, at small lattice constants an antiferromagnetic phase of γ-Fe prevails, and at large lattice constants a high-spin ferromagnetic phase is more stable.[10,13]

In order to investigate the origin of the remarkable increase in H_F at larger lattice constants, we have performed density-functional electronic-structure calculations for a 62-atom embedded cluster representing fcc Fe. Magnetic moments were obtained for several values of the lattice constant. Two phases were considered, ferromagnetic (FM) at larger interatomic distances, and antiferromagnetic (AFM) at smaller distances. The electronic spin density at the Fe nucleus obtained was used to calculate the hyperfine field.

In Sec. II, we briefly describe the method employed for the calculations, in Sec. III we present and discuss the results, and in Sec. IV we summarize our conclusions.

II. THEORETICAL METHOD

The cluster is of cubic geometry (see Fig. 1) and is embedded in the potential of several layers of neighbor atoms to simulate the external portion of the crystal. Several lattice constants were considered, varying from $a = 3.38$ to 3.77 Å. For smaller values, an antiferromagnetic phase consisting of alternating layers of up and down spins normal to the (001) direction was considered; for larger interatomic distances, we studied a ferromagnetic phase.

The first-principles self-consistent spin-polarized discrete variational method was employed[16] (DVM), in

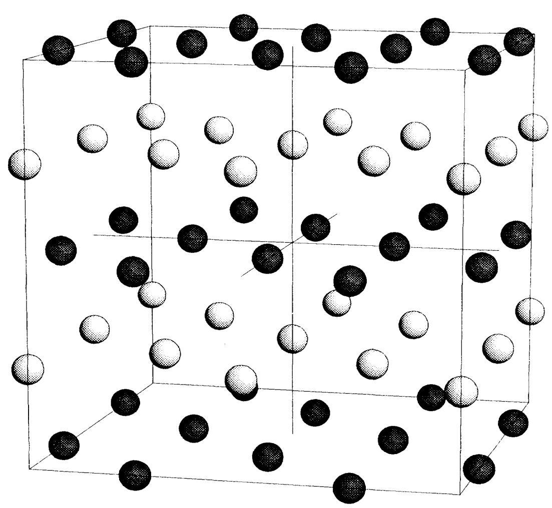

FIG. 1. 62-atom cluster representing fcc iron. Spheres of different shades are used to show more clearly the alternating layers of up and down spins of the antiferromagnetic phase.

the framework of density-functional theory.[17] The Kohn-Sham equations in the local-density approximation are solved self-consistently (in atomic units):

$$(-\nabla^2/2+V_c+V_{xc}^{\sigma})\phi_{i\sigma}=\varepsilon_{i\sigma}\phi_{i\sigma} , \tag{1}$$

where V_c is the Coulomb potential (nuclear and electronic) and V_{xc}^{σ} is the local exchange-correlation potential. Here, V_{xc}^{σ} was considered as given by von Barth and Hedin.[18] $\phi_{i\sigma}$ are the numerical cluster spin-orbitals from which is constructed the cluster spin-density for each spin σ:

$$\rho_{\sigma}(\mathbf{r})=\sum_i n_{i\sigma}|\phi_{i\sigma}(\mathbf{r})|^2 , \tag{2}$$

where $n_{i\sigma}$ is the occupation of cluster spin-orbital $\phi_{i\sigma}$.

In the construction of the potential in the Kohn-Sham Hamiltonian of Eq. (1), a model density is employed to facilitate the computation of the Coulomb terms.[16(b)] The model density is a multipolar expansion centered on the cluster nuclei, fitted by a least-squares procedure to the "exact" density; in the present calculations, only overlapping spherical terms were included, which is adequate for a compact metal. The functions $\phi_{i\sigma}$ are expanded on a basis of numerical atomic orbitals, obtained by local-density atomic calculations. The variational procedure leads to the conventional secular equations, which are solved self-consistently on a three-dimensional grid. This grid is random (diophantine)[16(a)] everywhere, except inside a sphere of radius $\sim$2.00 a.u. centered at the Fe nucleus where the hyperfine field is calculated. In this sphere, a regular grid is adopted for higher numerical precision. A total of $\sim$24 000 points is employed for this cluster.

The DVM cluster method has proved to be very useful in studying magnetic and hyperfine properties of several metallic systems.[19–22] Magnetic moments μ were obtained by subtracting the spin-up and spin-down electronic densities and integrating within the Wigner-Seitz sphere. The Fermi or contact hyperfine fields were obtained by the usual expression

$$H_c=8/3\pi\mu_B[\rho_{\uparrow}(0)-\rho_{\downarrow}(0)] , \tag{3}$$

where μ_B is the Bohr magneton and the term in brackets is the difference between the electronic density at the nucleus for spin up and spin down. The conduction electron contribution is obtained directly from the cluster valence eigenfunctions. The core electron contribution (1*s*, 2*s*, and 3*s*) is obtained in a separate local-spin-density calculation for the Fe atom, in which the radial potential is constructed from charge and spin densities as in the cluster. The dipolar contribution is zero by symmetry and the orbital contribution may be neglected, so the total field $H_F \cong H_c$. Both local properties μ and H_F are calculated at the innermost Fe atoms in the cluster, since they resemble most closely the atoms in bulk Fe.

III. RESULTS AND DISCUSSION

In Fig. 2 are plotted the computed values of μ for several Wigner-Seitz radii r_s. It may be seen that for the antiferromagnetic phase μ increases quite sharply with r_s. The high-spin ferromagnetic phase shows a much smaller rate of increase of μ with r_s. At $r_s=2.689$ a.u., which corresponds approximately to the value for which a sudden increase in H_F is experimentally observed, we have performed calculations for both antiferromagnetic and ferromagnetic configurations. At this point, a gap of $0.46\mu_B$ is present between μ in the ferromagnetic and antiferromagnetic phases; this, however, seems hardly likely to be responsible for the gap of approximately 300 KOe in H_F measured in the Mössbauer experiments. Incidentally, the values of μ obtained, as well as the inclination of the curves, agree reasonably well with results from band-structure calculation,[13] taking into account the different methodologies.

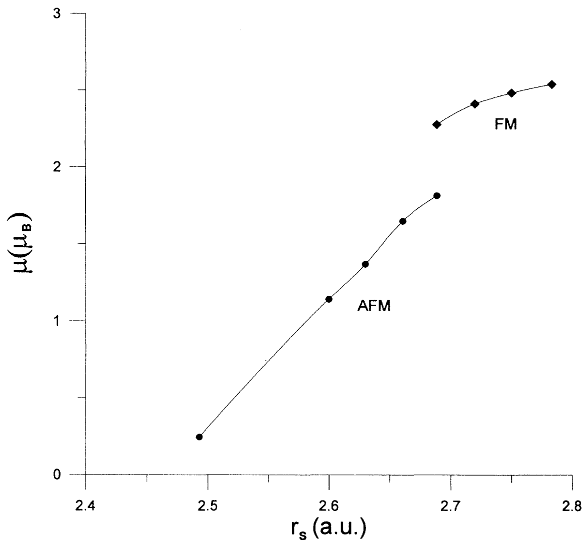

FIG. 2. Magnetic moments μ plotted against the Wigner-Seitz radius r_s for γ-Fe. AFM, antiferromagnetic; FM, ferromagnetic.

The theoretically obtained values of H_F are plotted against r_s in Fig. 3. The signs of H_F were not obtained experimentally. For the ferromagnetic phase, the calculated values agree well with experiment (Ref. 9). For the antiferromagnetic phase the magnitudes of the computed results are larger than those measured. However, it is clear that the predicted values of H_F for ferromagnetic and antiferromagnetic phases are separated by a large gap, as in the Mössbauer experiments.

The explanation for the apparent discrepancy between a large gap for H_F and a small gap for μ is obtained by examining Fig. 3. Here are also plotted separately the conduction electrons (4*s*) and core contributions to H_F. It may be observed that for the antiferromagnetic phase the conduction electrons give a positive contribution to H_F, which, added to the negative core contribution, results in H_F values of small magnitude. On the contrary, for the ferromagnetic phase the conduction electrons' contribution to H_F is negative as is the core contribution, so that those two add together to give a large value for $|H_F|$.

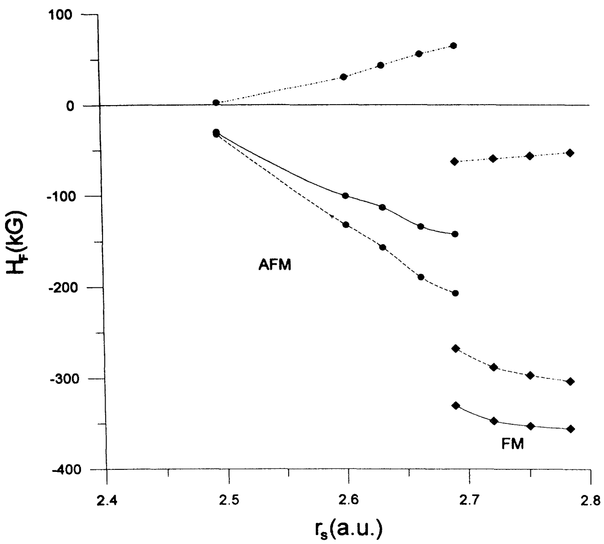

FIG. 3. Total hyperfine field H_F and components plotted against the Wigner-Seitz radius r_s. AFM, antiferromagnetic; FM, ferromagnetic. Conduction electrons' contribution, —·—·—·; core electrons' contribution, — — —; total, ——.

The cause of the different signs of the conduction electron contribution for ferromagnetic and antiferromagnetic γ-Fe is the difference in polarization of these electrons by the 3d moment. In the ferromagnetic case, the conduction (4s and 4p) electrons are polarized antiparallel to the 3d moment, which results in a larger 4s density at the nucleus for spin down than for spin up and thus a negative contribution to H_F [see Eq. (3)]. In the antiferromagnetic case, the conduction electrons are polarized parallel to the 3d moment, and thus the 4s gives a positive contribution to the spin density at the nucleus. To illustrate this point, calculated local magnetic moments for the AFM and FM phases are given in Table I, for values of r_s within the ranges studied, for 3d, 4s, and 4p orbitals of Fe. These were obtained by a Mulliken population analysis;[19,20] although this does not have quantitative value due to a certain degree of dependence on the basis set used, and on the choice of the manner of partitioning the overlap term, there is no ambiguity on the signs obtained.

From these results we may infer that the most probable cause for the discrepancy found between calculated and experimental values of H_F for the antiferromagnetic phase is that the conduction-electron contribution is somewhat underestimated in the calculation. Since the resulting H_F depends on a delicate balance between a positive and a negative term, a small error in the computed value of the positive conduction electrons' contribution, which is more difficult to obtain with precision, will be amplified in the final result.

TABLE I. Atomic orbital contributions to the local magnetic moment μ for AFM and FM fcc Fe (in μ_β).

	AFM[a]	FM[b]
3d	1.41	2.50
4s	0.04	−0.01
4p	0.05	−0.05

[a] $r_s = 2.63$ a.u.
[b] $r_s = 2.72$ a.u.

Recent neutron-scattering experiments for γ-Fe precipitates in Cu and Cu alloys have given evidence that the spin structure of antiferromagnetic γ-Fe has a spiral form,[23,24] more complex than the simple structure of alternating layers of up and down spins adopted here and deduced from earlier neutron-scattering experiments.[1] The spin structure, however, depends on the size of the particles measured. Nevertheless, the results presented here for the antiferromagnetic phase are generally valid, the μ and H_c values being subject to corrections if a more complex antiferromagnetic spin structure is actually present.

The calculations reported here are nonrelativistic, although the core electrons of Fe may be expected to present substantial relativistic effects. However, we estimate the nonrelativistic treatment to be sufficiently accurate since it has been demonstrated[25] that the contact hyperfine field is considerably less affected by the change of the wave functions due to the relativistic treatment, as compared, with example, with Mössbauer isomer shifts.

IV. CONCLUSIONS

To summarize, we conclude that the large difference observed experimentally in the magnitude of the hyperfine fields of antiferromagnetic and ferromagnetic γ-Fe originates mainly from different signs of the conduction-electron-contribution, which is positive for antiferromagnetic and negative for ferromagnetic, and not from large differences in the Fe magnetic moment in the two phases. This result shows clearly that the common practice of considering the hyperfine field as proportional to the magnetic moment may be very misleading.

ACKNOWLEDGMENTS

The authors thank Cassio Magnino and Marcelo Oliveira for the computer graphs. Calculations were performed at the Cray YMP of the Supercomputer Center of the Universidade Federal do Rio de Grande do Sul. Work supported in part by CNPq and by the U.S. National Science Foundation, through Grant No. INT92-02608 and through the MRC program at Northwestern University, Materials Research Center Grant No. 9120521.

[1]S. A. Abrahams, L. Guttman, and J. S. Kasper, Phys. Rev. **127**, 2052 (1962).
[2]P. Ehrhart, B. Schönfeld, H. H. Ettwig, and W. Pepperhoff, J. Magn. Magn. Mater. **22**, 79 (1980).
[3]B. Window, Philos. Mag. **26**, 681 (1972).
[4]G. J. Johanson, M. B. McGire, and D. A. Wheeler, Phys. Rev. B **1**, 3208 (1970).
[5]U. Gonser, C. J. Meechan, A. H. Muir, and H. Wiedersich, J. Appl. Phys. **34**, 2373 (1963).
[6]U. Gonser, K. Krischel, and S. Nasu, J. Magn. Magn. Mater. **15-18**, 1145 (1980).
[7]T. Ezawa, W. A. A. Macedo, U. Glos, W. Keune, K. P. Schletz, and U. Kirschbaum, Physica B **161**, 281 (1989).
[8]W. A. A. Macedo and W. Keune, Phys. Rev. Lett. **61**, 475 (1988).
[9]W. Keune, T. Ezawa, W. A. A. Macedo, U. Glos, and K. P. Schletz, Physica B **161**, 269 (1989).
[10]J. Kübler, Phys. Lett. **81A**, 81 (1981).
[11]D. Bagayoko and J. Callaway, Phys. Rev. B **28**, 5419 (1983).
[12]V. L. Moruzzi, P. M. Marcus, K. Schwarz, and P. Mohn, Phys. Rev. B **34**, 1784 (1986).
[13]C. S. Wang, B. M. Klein, and H. Krakauer, Phys. Rev. Lett. **54**, 1852 (1985).
[14]F. J. Pinski, J. Staunton, B. L. Gyorffy, D. D. Johnson, and G. M. Stocks, Phys. Rev. Lett. **56**, 2096 (1986).
[15]V. L. Moruzzi, P. M. Marcus, and J. Kübler, Phys. Rev. B **39**, 6957 (1989).
[16](a) D. E. Ellis and G. S. Painter, Phys. Rev. B **2**, 2887 (1970); D. E. Ellis, Int. J. Quant. Chem. Suppl. **2**, 35 (1968); (b) B. Delley and D. E. Ellis, J. Chem. Phys. **76**, 1949 (1982).
[17]See, for example: R. G. Parr and W. Yang, *Density Functional Theory of Atoms and Molecules* (Oxford University Press, New York, 1989).
[18]U. von Barth and L. Hedin, J. Phys. C **5**, 1629 (1972).
[19]H. Chacham, E. Galvão da Silva, D.Guenzburger, and D. E. Ellis, Phys. Rev. B **35**, 1602 (1987).
[20]D. Guenzburger, D. E. Ellis, and J. Danon, J. Magn. Magn. Mater. **59**, 139 (1986).
[21]D. Guenzburger and D. E. Ellis, Phys. Rev. Lett. **67**, 3832 (1991).
[22]D. Guenzburger and D. Ellis, Phys. Rev. B **49**, 6004 (1994).
[23]Y. Tsunoda, J. Phys.: Condens. Matter **1**, 10427 (1989).
[24]Y. Tsunoda, Y. Nishioka, and R. M. Nicklow, J. Magn. Magn. Mater. **128**, 133 (1993), and references therein.
[25]H. Akai, M. Akai, S. Blügel, B. Drittler, H. Ebert, K. Terakura, R. Zeller, and P. H. Dederichs, Prog. Theor. Phys. Suppl. **101**, 11 (1990), and references therein.